

pH-Responsive Diblock Copolymer Micelles at the Silica/Aqueous Solution Interface: Adsorption Kinetics and Equilibrium Studies

Kenichi Sakai,^{*,†} Emelyn G. Smith,[‡] Grant B. Webber,^{†,‡} Christophe Schatz,^{‡,#}
Erica J. Wanless,[‡] Vural Bütün,[§] Steven P. Armes,^{||} and Simon Biggs[†]

School of Process, Environmental and Materials Engineering, University of Leeds, Leeds LS2 9JT, United Kingdom, School of Environmental and Life Sciences, The University of Newcastle, Callaghan, N.S.W., 2308, Australia, Department of Chemistry, Eskisehir Osmangazi University, Campus of Meselik, Eskisehir 26040, Turkey, and Department of Chemistry, Dainton Building, The University of Sheffield, Brook Hill, Sheffield S3 7HF, United Kingdom

Received: May 9, 2006; In Final Form: June 1, 2006

The adsorption behavior of two examples of a weakly basic diblock copolymer, poly(2-(dimethylamino)ethyl methacrylate)-*block*-poly(2-(diethylamino)ethyl methacrylate) (PDMA-PDEA), at the silica/aqueous solution interface has been investigated using a quartz crystal microbalance with dissipation monitoring and an optical reflectometer. Dynamic and static light scattering measurements have also been carried out to assess aqueous solution properties of such pH-responsive copolymers. In alkaline solution, core-shell micelles are formed above the critical micelle concentration (cmc) by both copolymers, whereas the chains are molecularly dissolved (as unimers) at all concentrations in acidic solution. As a result, the adsorption behavior of PDMA-PDEA diblock copolymers on silica is strongly dependent on both the copolymer concentration and the solution pH. Below the cmc at pH 9, the cationic PDMA-PDEA copolymers adsorb as unimers and the conformation of the adsorbed polymer is essentially flat. At concentrations just above the cmc, the initial adsorption of copolymer onto the silica is dominated by the unimers due to their faster diffusion compared to the much larger micelles. Rearrangement of the adsorbed unimers and/or their subsequent displacement by micelles from solution is then observed during an equilibration period, and the final adsorbed mass is greater than that observed below the cmc. At concentrations well above the cmc, the much higher proportion of micelles in solution facilitates more effective competition for the surface at all stages of the adsorption process and no replacement of initially adsorbed unimers by micelles is evident. However, the adsorbed layer undergoes gradual rearrangement after initial adsorption. This relaxation is believed to result from a combination of further copolymer adsorption and swelling of the adsorbed layer.

Introduction

Understanding the interfacial adsorption of amphiphilic block copolymers is one of the most important topics in the field of materials science and engineering as a result of existing or proposed technological applications for nanostructured polymer films. These include uses as template structures for the secondary synthesis of microelectronic components, the preparation of surfaces with nanoscale variations in friction and adhesion, and possible uses in novel drug delivery systems. The use of amphiphilic block copolymers as the building blocks for self-assembled surface coatings having a high spatial order offers various advantages over the analogous small molecule surfactant coatings. For example, the rate of desorption of polymer chains adsorbed at a solid/solution interface is much slower than that of surfactants. It has already been reported that copolymer

coatings can improve various industrial products and processes, including paints, paper production, wastewater treatment, and mineral flotation. In addition, recent studies focusing on the self-assembly of amphiphilic block copolymers at the solid/aqueous solution interface have demonstrated their potential application in the world of nanotechnology, including as stimulus-responsive surface coatings,¹ nanostructured templates,^{2–5} and nanoreactors for preparing metal nanoparticles.^{6–9}

The adsorption behavior of amphiphilic diblock copolymer micelles from aqueous solution has been investigated extensively both theoretically¹⁰ and experimentally.^{11–15} For instance, Walter and co-workers reported the adsorption of a zwitterionic diblock copolymer poly(methacrylic acid)-*block*-poly(2-(dimethylamino)ethyl methacrylate) (PMAA-PDMA) on silica.^{11,13} It was shown that the adsorbed amount of this copolymer was strongly influenced by the solution pH and that direct adsorption of the copolymer micelles from solution can occur. An alternative adsorbed layer morphology has been reported by a number of other researchers:^{16–19} this consists of a brush-like conformation where the copolymer has a small anchor block adsorbed on the solid surface and a large “buoy” block extending into the solution phase.

When studying the adsorption of diblock copolymers, attention should not only be paid to the equilibrium state but also to the adsorption kinetics, which allows the adsorption mechanism

* To whom correspondence should be addressed. E-mail: k.sakai@leeds.ac.uk.

† University of Leeds.

‡ University of Newcastle.

§ Eskisehir Osmangazi University.

|| University of Sheffield.

[‡] Current address: Particulate Fluids Processing Centre, Department of Chemical and Biomolecular Engineering, The University of Melbourne, Parkville, Victoria, 3010, Australia.

[#] Current address: Laboratoire de Chimie des Polymères Organiques, LCPO (UMR5629) - ENSCPB, 16 Avenue Pey Berland, 33607 PESSAC cedex, France.

to be elucidated. Many studies of the adsorption kinetics of polymers are described in the literature. For example, Dijt and co-workers²⁰ reported the adsorption kinetics of nonionic poly(ethylene oxide) (PEO) onto silica in aqueous media by optical reflectometry (OR) and showed that the initial adsorption rate was determined by the maximal mass transfer rate from the bulk solution. Hoogeveen et al.²¹ also observed that the diffusion coefficient dictated the initial adsorption rate for strongly charged polyelectrolytes, e.g., quaternized poly(2-vinylpyridine) and quaternized poly(2-(dimethylamino)ethyl methacrylate), adsorbed onto silica and titania.

The complexity increases when considering the adsorption kinetics of diblock copolymer micelles, where the initial adsorption rate depends not only on the micellar diffusion but also on the exchange between free unimers and micelles in solution. Bijsterbosch and co-workers²² reported that, for copolymer micelles with a hydrophobic core of poly(dimethylsiloxane) and a hydrophilic corona of poly(2-ethyl-2-oxazoline), the adsorption kinetics onto silica were actually governed by the relatively fast dissociation of micelles into unimers *prior* to interfacial adsorption. The initial rate was shown to be a linear function of copolymer concentration, as expected. In situations where there is no (or very slow) unimer–micelle exchange in solution (e.g., kinetically “frozen” micelles), the adsorption kinetics are simplified, and post adsorption rearrangement/relaxation effects become important. Recently, adsorption of poly(*tert*-butylstyrene-*block*-sodium 4-styrenesulfonate) onto hydrophobic silica was reported.²³ When the initial micellar adsorption kinetics were compared with those of a star copolymer of similar composition, the aggregated block copolymer chains were found to relax and rearrange at the surface due to increased flexibility of individual chains within the micelles. Collectively these studies show that the degree of hydrophobicity, block length, and molecular weight have a profound effect on the micelle size and dynamics and consequently on their adsorption behavior at interfaces. Ultimately, improved understanding of the adsorption kinetics should enable better control over adsorption through appropriate copolymer design.

Improvements in synthetic methodology²⁴ now allow us to obtain copolymers that have well-controlled molecular weights and well-defined nanostructures. We have synthesized a series of stimulus-responsive diblock copolymers where one block is permanently hydrophilic and the other block is amphiphilic, that is, it can be made hydrophilic or hydrophobic depending on the solution pH.^{25–29} For example, diblock poly(2-(dimethylamino)ethyl methacrylate)-*block*-poly(2-(diethylamino)ethyl methacrylate) (PDMA-PDEA) copolymers can form pH-responsive micelles reversibly in aqueous solution: PDMA-PDEA exists as molecularly dissolved chains or unimers in acidic solution, while in alkaline solution core–shell micelles are formed, with the hydrophobic PDEA chains located in the cores and the weakly hydrophilic PDMA chains forming the micelle coronas.^{25,26,29} This micellization behavior has previously enabled us to report the preparation of stimulus-responsive micelle monolayers at the solid/aqueous solution interface.^{30–32} Although these equilibrium observations provide possibilities for using these copolymers as building blocks for surface coatings, little quantitative data has been obtained to date, particularly in the early stages of adsorption.

Herein the adsorption of two PDMA-PDEA diblock copolymers at the silica/aqueous solution interface is examined as a function of solution pH, block ratio, and copolymer concentra-

TABLE 1: Molecular Characteristics of the Copolymers Investigated

| | DMA content ^a mol % | M_n^b g·mol ⁻¹ | polydispersity index ^b |
|---|-----------------------------------|-----------------------------|--------------------------------------|
| PDMA ₁₀₀ | 100 | 17 600 | 1.09 |
| PDMA ₉₆ -PDEA ₂₆ | 79 | 21 800 | 1.09 |
| PDMA ₉₃ -PDEA ₂₄ ^c | 79 | 19 100 | 1.13 |
| PDMA ₅₄ -PDEA ₂₄ | 69 | 13 000 | 1.18 |

^a As determined by ¹H NMR spectroscopy. ^b As determined by GPC calibrated with poly(methyl methacrylate) standards. ^c This diblock copolymer was used for the OR and SLS measurements. This copolymer is almost identical with PDMA₉₆-PDEA₂₆ in terms of its molecular characteristics. The subscripts refer to the mean degrees of polymerization of each block. The term PDMA_{9X}-PDEA_{2Y} is used as a general name for these equivalent copolymers.

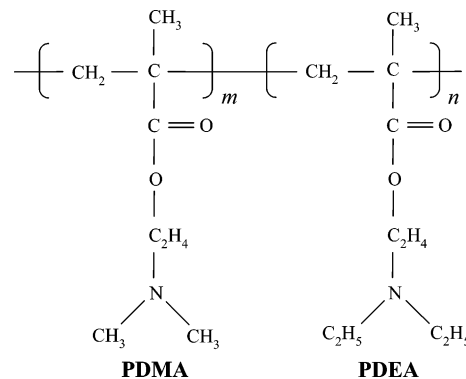


Figure 1. Chemical structure of the PDMA_m-PDEA_n diblock copolymer.

tion. A quartz crystal microbalance with dissipation monitoring (QCM-D) was used in order to evaluate the viscoelastic nature of the adsorbed copolymer layer formed on silica, as well as the extent of adsorption. It is well known that the mass measured using the QCM technique includes the mass of solvent molecules (in this case water) associated with the adsorbed materials.^{33–37} Thus, complementary measurements using OR were carried out in order to determine the actual adsorbed amount of copolymer and hence allow estimation of the degrees of hydration of the adsorbed copolymer layers from the combined data.

Experimental Section

Materials. The PDMA homopolymer and the three PDMA-PDEA diblock copolymers described in Table 1 were synthesized using either group-transfer polymerization (GTP)²⁹ or atom-transfer radical polymerization (ATRP).³⁸ The chemical structure of PDMA-PDEA is shown in Figure 1. The molecular weights and the polydispersity indices of the copolymers were measured using gel permeation chromatography (GPC) with a THF eluent at a flow rate of 1.0 cm³·min⁻¹. Calibration was carried out with poly(methyl methacrylate) standards. Block compositions were estimated using ¹H NMR spectroscopy.

Silicon wafers (purchased from Silicon Valley Microelectronics, CA with a premeasured thermal oxide layer of 115 nm) were used for the OR measurements. All other reagents were of analytical grade and water was Millipore Milli-Q grade.

Measurements. (I) QCM-D. A commercial (Q-Sense, Göteborg, Sweden) QCM-D was used to measure adsorbed amounts of PDMA₉₆-PDEA₂₆ and PDMA₅₄-PDEA₂₄ on silica. The features of this instrument are described in greater detail elsewhere.^{39,40} In a typical QCM experiment, the resonant frequency of an AT-cut piezoelectric quartz crystal is monitored as it changes due to adsorption of materials onto the substrate. The adsorbed mass can then be calculated by applying the

Sauerbrey equation⁴¹

$$\Delta f = -\frac{f_0^2}{\rho_q \nu_q} \Delta m = -\frac{f_0}{\rho_q t_q} \Delta m = -C \Delta m \quad (1)$$

where Δf is the change in resonant frequency, f_0 is the resonant frequency of the “clean” substrate, ρ_q and ν_q are the specific density and shear wave velocity of the quartz respectively, t_q is the thickness of the quartz crystal and Δm is the mass of material adsorbed. It is noted that the mass measured using the QCM technique is the total mass of material coupled to the oscillation. Consequently, solvent molecules that are bound to or occluded within the adsorbed layer will also contribute to the measured mass and adsorbed amounts determined using QCM typically exceed those measured using other analytical techniques such as ellipsometry,^{33,34} X-ray photoelectron spectroscopy,³⁵ surface plasmon resonance,³⁶ or OR.³⁷

An additional feature of the Q-Sense quartz crystal microbalance is the simultaneous measurement of dissipation. Here, the voltage driving the oscillation of the crystal is turned off, and the decay of the oscillation is monitored. For a rigid layer, the decay is relatively slow, while for a viscoelastic layer the decay is fast, due to the dampening effect of the adsorbed layer. Thus, by comparing dissipation values it is possible to assess the *relative* rheological properties of adsorbed layers. The QCM-D data presented here are those measured at the third overtone (~15 MHz); this overtone offers better signal-to-noise than the fundamental frequency and is less affected by the cell mounting than higher overtones. These data were also used in calculations involving the Sauerbrey equation.

A single sensor crystal with a silica coating was used for all QCM-D experiments. Prior to these measurements, the crystal was ultrasonicated for 15 min in an anionic/nonionic surfactant mixture (Decon 90, Decon Laboratories Ltd., UK), rinsed with water, cleaned using UV irradiation (approximately 9 mW·cm⁻² at 254 nm) for at least 10 min, and finally rinsed thoroughly with water again. The rubber O-ring which seals the cell/sensor assembly was also ultrasonicated for 15 min in Decon 90 solution followed by a thorough Milli-Q water rinse. After washing, the sensor and the O-ring were assembled in the QCM-D instrument and Milli-Q water was injected into the sensor cell. The frequency and dissipation values were monitored to assess the cleanliness of the sensor. When the sensor was deemed to be clean, the water was replaced by a solution containing 10 mmol·dm⁻³ background electrolyte at the desired pH of the copolymer solution to be studied, and the system was allowed to stand for at least 1 h. This enabled the silica surface charge to equilibrate with the solution pH, and also allowed the measurement cell to “settle” after assembly. Experience has shown that the values of resonant frequency and dissipation, across all overtones, drift in the period immediately after assembly. This is most likely due to thermal fluctuations and relaxation of the O-ring.⁴² Injection of copolymer solution was made only after a stable baseline in the electrolyte solution was achieved. The equilibration time was 10 h after the injection of each sample copolymer solution. All measurements were performed at a constant temperature of 25.0 °C. The error for the adsorbed amount and dissipation determined from a typical QCM-D experiment is estimated to be ±20%.

(II) Optical Reflectometry. The silicon wafers were kept in a dust-free environment and subjected to a three-step treatment before use. This involved UV irradiation for 30 min, followed by ultrasonication in ethanol for 20 min. The silica was then stored in ethanol, rinsed just prior to use with Milli-Q water,

soaked in 10 wt % aqueous NaOH for 10 min, followed by copious amounts of Milli-Q water to give an hydroxylated silica surface. A fresh piece of silica was used for each experiment and discarded thereafter.

Copolymer adsorption to silica was measured by OR as described by Dijt and co-workers;⁴³ our instrumentation has been described in detail in a previous paper.⁴⁴ Briefly, this technique involves measuring the change in reflective properties of a substrate as it adsorbs to the surface. A stagnation point flow cell with well-defined hydrodynamics is used where diffusion is the only transport mechanism to the surface. A typical experiment involves the copolymer being introduced from a gravity fed line through a two-way valve after the surface has equilibrated to the desired pH and ionic strength and a stable baseline has been recorded. Continuous adsorption measurements were taken from the change in the ratio of the *s* and *p* polarizations of the reflected laser beam over long time intervals with temporal resolution of <0.1 s. The change in ratio of the output signal (ΔS) was converted to an adsorbed amount (Γ_{OR}) using eq 2

$$\Gamma_{\text{OR}} = \frac{\Delta S}{S_0} \frac{1}{A_s} \quad (2)$$

where S_0 is the initial output value and A_s is the sensitivity factor, which is calculated from the optical properties of each component in the system. The instrument was housed in an incubator at 25 ± 2 °C. The error for the adsorbed amount determined from a typical OR experiment is estimated to be ±10%.

(III) Dynamic Light Scattering (DLS). A Malvern NanoSeries ZetaSizer Nano-ZS (Malvern Instruments, UK) equipped with a Helium–Neon laser source (wavelength 633 nm; power 4.0 mW) was used for measuring the micelle size of the diblock copolymers in bulk solution. Scattering data were collected for at least 100 individual measurements at a constant scattering angle and averaged for each sample. The obtained scattering data were fitted using a number-weighted cumulative analysis to estimate the diffusion coefficient of the copolymer micelles in solution (D_{sol}). The hydrodynamic diameter of the micelles (D_{H}) is obtained by using the Stokes–Einstein equation⁴⁵

$$D_{\text{H}} = \frac{k_{\text{B}} T}{3\pi\eta D_{\text{sol}}} \quad (3)$$

where k_{B} is the Boltzmann constant, T is the absolute temperature, and η is the viscosity of the solution.

(IV) Static Light Scattering (SLS). SLS was used to determine the aggregation number (N_{agg}) from the weight-average molecular weight (M_{w}) of the micelles. SLS measurements were processed in batch mode using a nonthermostated multi-angle laser light scattering photometer (Wyatt, Dawn EOS, CA) equipped with a 25-mW Ga/As laser beam operating at the wavelength of 683 nm. Light-scattering intensities recorded at 18 angles between 23 and 147° were derived using the ASTRA software according to the Zimm procedure. This involves plotting Kc/R_{θ} vs $\sin^2(\theta/2) + kc$, where K is an optical constant that contains the specific refractive index increment dn/dc , c is the copolymer concentration (mg·cm⁻³), R_{θ} is the Rayleigh ratio, k is an arbitrary constant for the convenient graphical representation of the Zimm plot, and θ is the scattering angle, respectively. Double extrapolation to zero angle and to zero concentration yielded the value of M_{w} . For each measurement, five different copolymer concentrations were prepared by serial dilution using known weights of Borax buffer solution (10 mmol·dm⁻³) of equal pH. Both these buffered copolymer

solutions and the solvent were directly filtered using a 0.20 μm filter membrane (GHP Acrodisc, Pall Gelman Science, MI) into the light scattering cells. Refractive index increments (dn/dc) were determined independently with an interferometric refractometer (Wyatt, Optilab DSP, CA) operating at a wavelength of 690 nm. All measurements were made at 24 ± 2 °C. The overall error in the weight-average molecular weights and the micelle aggregation numbers estimated by SLS was estimated to be approximately $\pm 10\%$.

Results and Discussion

(I) Micellar Characteristics. For characterizing the adsorption behavior of PDMA-PDEA at the silica/aqueous solution interface, it is important to understand the aqueous solution properties in advance. As noted earlier, we have already investigated the micellization behavior of various PDMA-PDEA diblock copolymers in bulk solution as a function of the solution pH.^{25,26,29,32} However, we have not studied the relationship between copolymer concentration and the solution and/or surface properties of these PDMA-PDEA copolymers. Therefore, in this study, micelle size measurements were performed using DLS in order to determine the critical micelle concentration (cmc).

Our measurements were carried out at a constant solution pH of 9 in the presence of $10 \text{ mmol}\cdot\text{dm}^{-3}$ KNO_3 as a background electrolyte. Within the resolution of our experimental setup, no signals corresponding to micellar aggregates were detected below 20 ppm for PDMA_{9X}-PDEA_{2Y} and below 10 ppm for PDMA₅₄-PDEA₂₄, respectively. In contrast, clear evidence of micelle formation was obtained above these concentrations. Intensity-average micellar diameters were determined to be 22–27 nm for PDMA_{9X}-PDEA_{2Y} and 25–30 nm for PDMA₅₄-PDEA₂₄, respectively. Bütün and co-workers²⁹ have reported that the micelle diameter of PDMA-PDEA copolymers above the critical micellization pH is mainly influenced by the following two factors: the overall copolymer molecular weight and the block composition. An increase in copolymer molecular weight at a fixed DMA content will lead to larger micelles being formed. Similarly, larger micelles are also obtained when the DMA content is reduced for a given copolymer molecular weight. Our current results suggest that slightly larger PDMA₅₄-PDEA₂₄ micelles are formed due to this copolymer's reduced (actual and relative) DMA content.

To further clarify the micellar characteristics, the N_{agg} of the micelles was estimated using SLS. These measurements were performed in $10 \text{ mmol}\cdot\text{dm}^{-3}$ Borax buffer solutions to ensure pH stability. It was estimated that the N_{agg} of PDMA_{9X}-PDEA_{2Y} at pH 8.5 was 42 ± 3^{46} and that of PDMA₅₄-PDEA₂₄ at pH 9 was 92 ± 7 , respectively. Since the relative DMA content of PDMA₅₄-PDEA₂₄ is less than that of PDMA_{9X}-PDEA_{2Y}, the former copolymer is more hydrophobic than the latter. Thus the greater hydrophobicity of PDMA₅₄-PDEA₂₄ leads to a higher aggregation number but only a slightly larger micelle diameter; note that the molecular weight of PDMA₅₄-PDEA₂₄ is also significantly lower than that of PDMA_{9X}-PDEA_{2Y} (see Table 1). Similar results have been reported in the literature.⁴⁷

By use of the micelle diameters and the N_{agg} values, the water contents of the diblock copolymer micelles were estimated. In our calculation, we assumed that (i) the overall micelle density is $1.1 \times 10^3 \text{ kg}\cdot\text{m}^{-3}$ and (ii) the PDEA core blocks are completely dehydrated at pH 9.²⁹ For example, since the mass of each PDMA_{9X}-PDEA_{2Y} copolymer micelle is $6.5 \times 10^{-21} \text{ kg}$, the mean degree of hydration (or water content) is estimated to be around 79 wt % (the mass of the PDEA core chains is $3.4 \times 10^{-22} \text{ kg}$ per micelle and the mass of the PDMA coronal

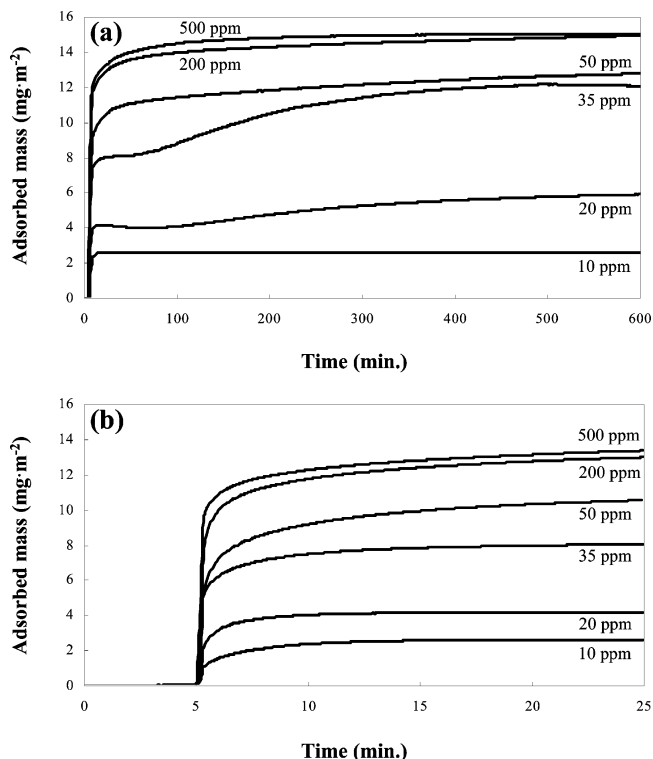


Figure 2. Adsorption kinetics of PDMA_{9X}-PDEA_{2Y} on silica monitored with QCM-D. The solution pH was set to 9 in the presence of $10 \text{ mmol}\cdot\text{dm}^{-3}$ KNO_3 . The copolymer solutions were injected at 5 min. (a) Gives the kinetics over a prolonged period of adsorption, while (b) shows the same data on a short time scale.

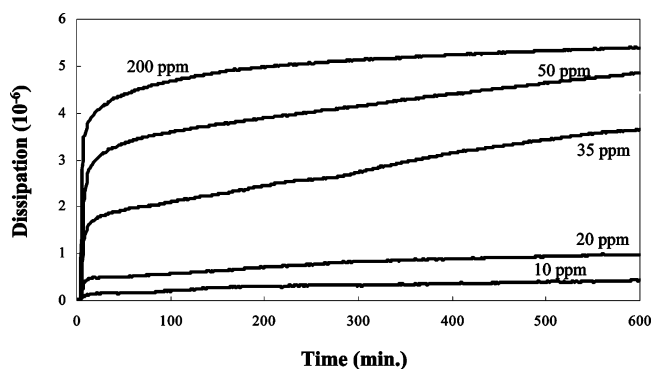


Figure 3. Change in dissipation for adsorption of PDMA_{9X}-PDEA_{2Y} on silica monitored with QCM-D. The solution pH was set to 9 in the presence of $10 \text{ mmol}\cdot\text{dm}^{-3}$ KNO_3 .

chains is $1.1 \times 10^{-21} \text{ kg}$ per micelle). Similarly, the mean degree of hydration of the PDMA₅₄-PDEA₂₄ micelles is estimated to be slightly higher at 86 wt %.

We also carried out DLS measurements at pH 4. The scattered light intensity was very low at or below 500 ppm, indicating dissociation of the micelles to form molecularly dissolved copolymer chains. This was expected, since the critical micellization pH of these copolymers is approximately 7–8.³²

(II) Adsorption Kinetics of PDMA-PDEA at pH 9. Figures 2 and 3 present typical QCM-D results for the adsorption of PDMA_{9X}-PDEA_{2Y} at the silica/aqueous solution interface at pH 9. The change in mass as a function of time and at a range of copolymer concentrations is shown in Figure 2, while the corresponding dissipation changes are given in Figure 3. The solutions contain $10 \text{ mmol}\cdot\text{dm}^{-3}$ KNO_3 background electrolyte. It is clear from these figures that the results are strongly dependent on the initial copolymer concentration. In the analysis

that follows, the discussion will focus on three concentration regimes: (i) below the cmc, (ii) just above the cmc, and (iii) well above the cmc.

At low copolymer concentrations, it is generally accepted that adsorption of neutral diblock copolymers onto surfaces from nonpolar solvents is a two-stage process.^{19,48–50} The first stage involves diffusion of the copolymer chains to the solid surface, with accompanying rapid adsorption. The second (slow) stage involves a change in the conformation of the adsorbed copolymer chains due to the repulsive osmotic pressure between overlapping polymer chains on the surface. As a result, the adsorbed copolymer adopts a brush-like conformation at the solid/solution interface. This two-stage adsorption process may also be applicable on short time scales (Figure 2b) to the present study.

For example, at a concentration of 10 ppm the adsorbed mass increases sharply in the early stages of adsorption. Then, the rate of increase in the adsorbed mass gradually slows before a final plateau value is attained. DLS measurements suggest that the cmc of this diblock copolymer is around 20 ppm, hence PDMA_{9X}-PDEA_{2Y} should adsorb exclusively as individual chains (unimers) from a 10 ppm solution. The driving force for adsorption is believed to be due to the electrostatic attraction between the weakly cationic PDMA coronal chains and the anionic silica surface.

Once a critical coverage is attained, the existing adsorbed layer will prevent any further adsorption without an associated conformational change such as the development of a brush-like film. The two-stage adsorption process described above requires that the adsorbed copolymer chains, which initially lie relatively flat, become partially desorbed from the interface. Since the hydrophilic character of PDMA chains is significantly higher than that of PDEA chains at pH 9, the PDMA chains most likely become selectively desorbed from the silica surface to act as a “buoy” block, while the PDEA chains remain firmly anchored at the interface. However, our dissipation data indicate an equilibrium value of less than 0.5×10^{-6} (Figure 3), suggesting that the adsorbed layer retains a flat, rather than brush-like, conformation. Furthermore, it is interesting to note that this dissipation value is similar to that observed for adsorption of PDMA₁₀₀ homopolymer from a 500 ppm solution onto the silica surface at pH 9 (0.4×10^{-6} , data not shown). Similarly, the corresponding adsorbed mass of PDMA₁₀₀ from 500 ppm solution ($3.0 \text{ mg}\cdot\text{m}^{-2}$) is consistent with the adsorbed mass of PDMA_{9X}-PDEA_{2Y} from 10 ppm solution ($2.6 \text{ mg}\cdot\text{m}^{-2}$). Since PDMA₁₀₀ behaves as a weak polyelectrolyte at this pH (with $\text{p}K_a \approx 7$),²⁹ it is expected to adsorb in a flat conformation on an oppositely charged surface.^{51,52} It is therefore reasonable to assume that the adsorption of PDMA_{9X}-PDEA_{2Y} unimers results in a relatively thin adsorbed monolayer.

The analysis of kinetic data collected *above* the cmc is more complex because of the presence of copolymer micelles. In fact, at 20 ppm PDMA_{9X}-PDEA_{2Y}, the adsorbed mass measured by QCM-D increases sigmoidally with time (Figure 2a). The adsorbed mass initially reaches a pseudo-plateau within 10–15 min after injection of the copolymer solution, before exhibiting a further gradual increase toward a final plateau value over 10 h. Similar adsorption behavior was also observed at a concentration of 35 ppm. On the other hand, above 50 ppm the adsorbed mass exhibits a slow monotonic increase after the initial sharp increase. Interestingly, the corresponding dissipation also increases continuously over the same time scale (Figure 3).

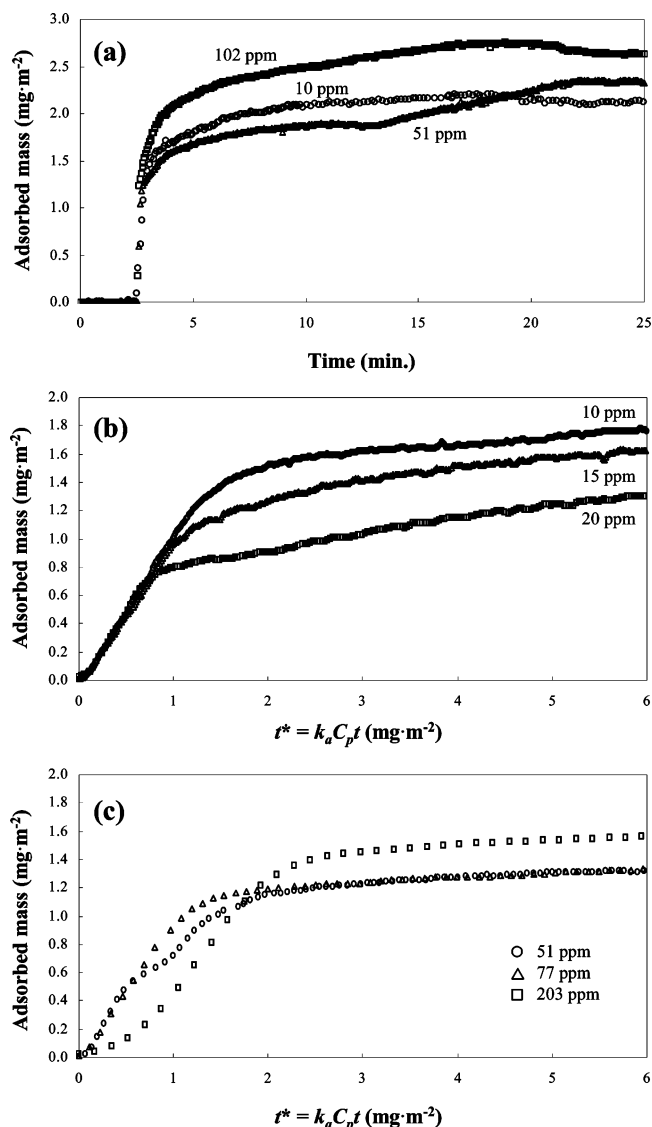


Figure 4. Adsorption kinetics of PDMA_{9X}-PDEA_{2Y} on silica monitored with OR. The solution pH was set to 9 in the presence of $10 \text{ mmol}\cdot\text{dm}^{-3}$ KNO₃. The copolymer solutions were injected at 2.5 min. (a) Gives change in the adsorbed mass as a function of time, while (b) and (c) show the same results re-scaled as a function of normalized time $t^* = k_a C_p t$.

Figure 4a shows the typical kinetic data obtained from OR for the adsorption of the PDMA_{9X}-PDEA_{2Y} copolymer at each of the three concentration regimes outlined above. These data were collected over a 20-min period after replacement of the solution containing the background electrolyte at pH 9 with the copolymer solution of interest. Therefore, these results correspond to the QCM-D results shown in Figure 2b. Like the QCM-D study, the OR data obtained using 51 ppm copolymer show a pseudoplateau over time-scales of 5–12 min (the copolymer was injected at 2.5 min), after which the adsorbed amount increases further to reach an equilibrium value after 23 min. Given these QCM-D and OR data for the concentration regime just above the cmc, we propose a structural rearrangement in the adsorbed layer due to the presence of both unimers and micelles in solution.

Closer examination of the OR kinetic data is made in parts b and c of Figure 4, where the effect of the cmc of this copolymer on the adsorption kinetics is readily apparent over short time-scales. Here, the data are presented using a rescaled time axis (t^*), according to the approach of Toomey et al.,²³

where $t^* = k_a c_p t$ and c_p and k_a are the copolymer concentration and the rate constant determined from the maximum initial rate of adsorption, respectively. This rescaling facilitates comparison between data collected at widely varying initial concentrations, as reported here. In Figure 4b, the first point to make is that the initial slope is unity, which signifies that the adsorption kinetics are diffusion limited and that adsorption is very efficient, i.e., that each molecule reaching the surface becomes adsorbed. It is also apparent from Figure 4b that once again we observe a qualitative change in the adsorption kinetics in the vicinity of the copolymer cmc. Below the cmc, the curves are characteristic of a single process, with a rapid increase to a single plateau value. However, deviation from the unit slope is observed for 20 ppm copolymer at a lower adsorbed amount ($0.8 \text{ mg}\cdot\text{m}^{-2}$) with a small upward inflection on the re-scaled time axis at $t^* = 2 \text{ mg}\cdot\text{m}^{-2}$. We attribute this to the initial rapid adsorption of unimers, followed by a contribution from more slowly diffusing micelles. These kinetic data resemble the QCM-D data shown in Figure 2b, although here the transition occurs on a shorter time-scale. We attribute this time variation to important differences between the two techniques: OR detects the copolymer alone while the QCM-D data necessarily include entrained water; moreover, the flow conditions used for the two techniques are fundamentally different. Interestingly, the equilibrium adsorbed amount obtained for PDMA₈₅ homopolymer (data not shown) is approximately $0.98 \text{ mg}\cdot\text{m}^{-2}$ and the maximum adsorbed amount is attained within a much shorter time scale. Comparison to the data obtained just above the cmc, where the deviations from the unit slope occur between $t^* = 1.0$ and $1.5 \text{ mg}\cdot\text{m}^{-2}$ on the rescaled time axis, suggests that exposed hydrophobic PDEA chains facilitate surface rearrangements to allow higher equilibrium adsorbed amounts of $\sim 2.3 \text{ mg}\cdot\text{m}^{-2}$ to be attained.

In Figure 4c, rescaled kinetic data are shown for the concentration region above the cmc. Deviation from the unit slope occurs at an even lower adsorbed amount ($0.5 \text{ mg}\cdot\text{m}^{-2}$) for 51 ppm copolymer than for 20 ppm copolymer due to individual chains still contributing to the adsorption process which is now dominated by the increased micelle concentration. At 77 ppm copolymer, a single adsorption process (now solely due to micelles) dominates the observed kinetics. The unit slope observed here signifies that the copolymer adsorption is once again diffusion limited. For concentrations far above the cmc, for example at 203 ppm, this gradient is less than unity. This signifies that, at such a high copolymer micelle concentration, not every species is adsorbed at the surface due to the competition for available surface sites.

During the initial rapid adsorption stage, the diffusion coefficient of the copolymer toward the surface (D_{surf}) can be related to the adsorbed amount using the following equation⁴⁸

$$\Gamma(t) = 2C_p \sqrt{\frac{D_{\text{surf}} t}{\pi}} \quad (4)$$

where $\Gamma(t)$ is the adsorbed amount at time t and C_p is the concentration of the diblock copolymer in solution. This relationship assumes that each copolymer reaching the solid surface is immediately adsorbed. In addition, D_{surf} necessarily differs from the diffusion coefficient of the diblock copolymers in solution (D_{sol}) estimated from DLS measurements, since D_{surf} must also include any interactions between the copolymer and the surface that may influence interfacial adsorption.

Figure 5 presents the D_{surf} data calculated using the maximum slope of the OR adsorption kinetics plot for the diblock

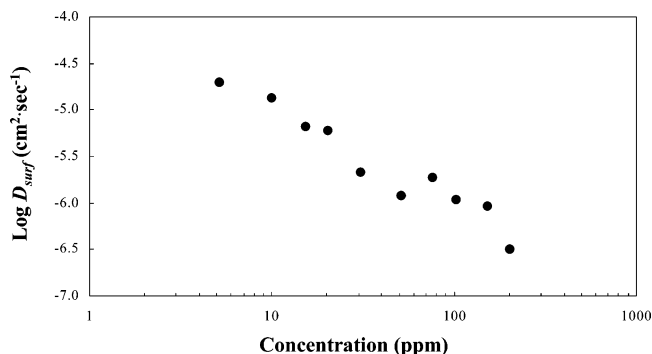


Figure 5. Diffusion coefficient of the copolymers onto silica in the presence of $10 \text{ mmol}\cdot\text{dm}^{-3} \text{ KNO}_3$ at pH 9.

PDMA_{9X}-PDEA_{2Y} copolymer on silica at pH 9 as a function of the square root of time (data not shown). These values range from 3.2×10^{-7} to $2.0 \times 10^{-5} \text{ cm}^2\cdot\text{s}^{-1}$. The D_{sol} value of this copolymer is calculated to be $2.0 \times 10^{-7} \text{ cm}^2\cdot\text{s}^{-1}$ at pH 9. Thus, the D_{surf} values are generally higher than the D_{sol} value, implying that there is a strong attractive interaction between the copolymer and the surface during initial adsorption. Furthermore, the D_{surf} values decrease linearly with increasing concentration. This linear relationship in a $\log D_{\text{surf}}$ vs $\log C_p$ plot has also been reported by Walter and co-workers¹¹ for the adsorption kinetics of negatively charged diblock PMAA-PDMA copolymers onto negatively charged silica at neutral pH. However, the reported D_{surf} values by Walter and co-workers¹¹ are significantly smaller than the values given in Figure 5 at the same copolymer concentrations (in $\mu\text{mol}\cdot\text{dm}^{-3}$). This difference can be rationalized as follows: (i) both the molecular weight and the size of the micellar aggregates in solution of the PMAA-PDMA copolymer employed in their work are larger than those of the PDMA_{9X}-PDEA_{2Y} copolymer examined here and (ii) the adsorption of PDMA_{9X}-PDEA_{2Y} is enhanced by a strong electrostatic attraction, which is not a feature of the system reported by Walter and co-workers.¹¹

The QCM-D and OR data indicate competitive adsorption between unimers and micelles in micellar solutions of PDMA_{9X}-PDEA_{2Y}. The correct interpretation of these kinetic data requires analysis of both the initial stages and also the longer time-scale behavior (on which rearrangement and/or replacement of adsorbed copolymer occurs).

At concentrations just above the cmc the adsorbed mass increases further after initially reaching a pseudoplateau (see Figures 2 and 4). The corresponding dissipation data from the QCM-D (Figure 3) do not exhibit well-defined plateau regions; instead, dissipation increases continuously throughout the experiment. These results suggest that the adsorbed layer undergoes some type of conformational rearrangement after an initial adsorption phase. Consideration of the data from this regime suggests two possible mechanisms: either (i) initial adsorption of unimers and subsequent exchange for micelles or (ii) initial unimer adsorption followed by a surface micellization process (driven by the further adsorption of unimers from solution and supplied by micelle dissociation in the interfacial zone).

Dijt and co-workers⁵³ investigated competitive adsorption between two kinds of PEO having two different chain lengths. It was shown that the initially adsorbed short PEO chains were ultimately replaced by longer PEO chains. It is noteworthy that the observed displacement kinetics closely resembles the kinetic data described in the present work. According to Dijt and co-workers,⁵³ the first plateau corresponds to the saturation level that is characteristic of the adsorption of the shorter PEO chains

while the final plateau equates to the saturated amount for the larger PEO species. Entropy provides the driving force for this chain exchange since longer chains lose less overall entropy when adsorbed at the interface; displacement simply occurs because the shorter chains diffuse to the interface more quickly. By assumption that the same adsorption mechanism applies to our system, the observed pseudoplateau indicates the saturation level for unimer adsorption and the final plateau corresponds to the complete displacement of these unimers by micelles.

Another possible explanation for the observed two-stage adsorption kinetics is surface micellization. Once the direct adsorption of unimers occurs at the solid/aqueous solution interface, further adsorption of unimers might be facilitated in order to avoid an energetically unfavorable contact of the hydrophobic PDEA chains to the solution phase. As a result, rearrangement of the adsorbed layer occurs via the further adsorption of unimers; in this scenario, the micelles merely serve as a reservoir for the unimers. In our previous investigation, the aggregation number of the adsorbed PDMA_{9X}-PDEA_{2Y} micelles on silica was estimated to be greater than that of the micelles in solution.⁴⁶ This experimental result may be rationalized more easily by invoking surface micellization, rather than the displacement of unimers by micelles. It is noted that the initial adsorption of unimers on silica is driven by electrostatic attraction and (possibly) the hydrophobic character of the PDEA chains, whereas the further unimer adsorption results from the hydrophobic interaction induced by exposed PDEA. As a result, the adsorption rates for the two processes are expected to differ, although the diffusion rate of unimers in solution must be constant during the overall adsorption period. However, it is difficult to rationalize the observation of an intermediate adsorption plateau using this model, since we might expect further adsorption to proceed simultaneously (and competitively) with initial unimer adsorption. A fuller understanding of the adsorption data, although highly desirable, is more challenging than originally anticipated. Further work on the conformational changes within the adsorbed layer as a function of time using in situ atomic force microscopy may provide further insights. However, so far we have not had any success in obtaining high quality images during the initial stages of adsorption.

Far above the cmc, both the adsorbed amount and the dissipation increase continuously over the whole time scale investigated. As already noted, free micelles compete effectively with individual copolymer chains for adsorption onto the silica at these higher concentrations, thus micelles are expected to be involved even during the initial stages of adsorption. Once adsorbed onto silica, the micelles undergo conformational relaxation in order to saturate any local anionic charge, to minimize repulsion between neighboring micelles, and to facilitate further adsorption. If additional adsorption occurs, it should result in an increase in the mean aggregation number for the adsorbed micelles compared to that for micelles in solution.⁴⁶ The kinetic data suggest that relaxation of the adsorbed layer and any associated additional adsorption occur over time-scales of several hours. These adsorption mechanisms are summarized schematically in Figure 6.

(III) Adsorption Isotherm of PDMA-PDEA at pH 9. Figure 7 shows the adsorption isotherms of PDMA_{9X}-PDEA_{2Y} using either QCM-D or OR at pH 9 in the presence of 10 mmol·dm⁻³ KNO₃. It is apparent from this Figure that the two isotherms are logically quite different: that obtained by OR has a plateau value of 2.5 mg·m⁻² above a copolymer concentration of 30 ppm, whereas the adsorbed amount monitored by QCM-D (including entrained water) increases more gradually with

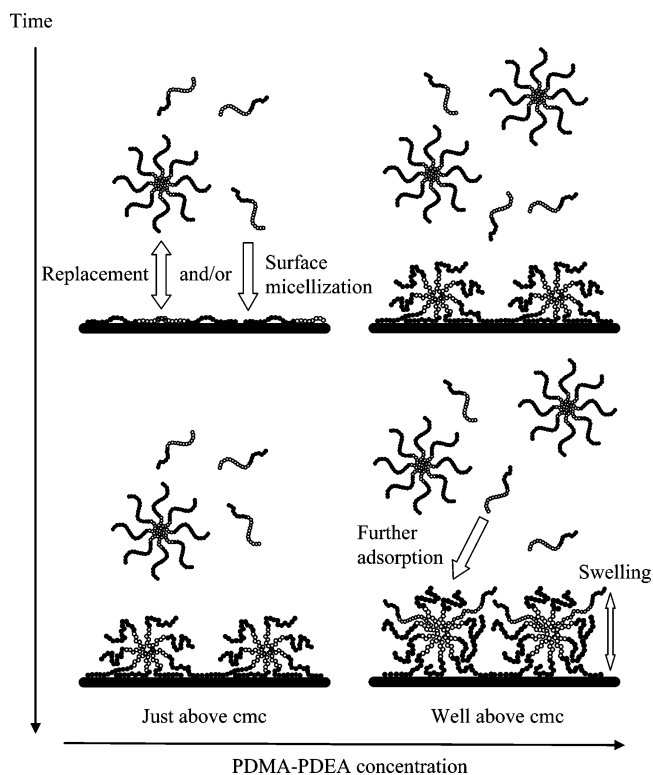


Figure 6. Schematic representation of the adsorption of PDMA-PDEA copolymer onto silica.

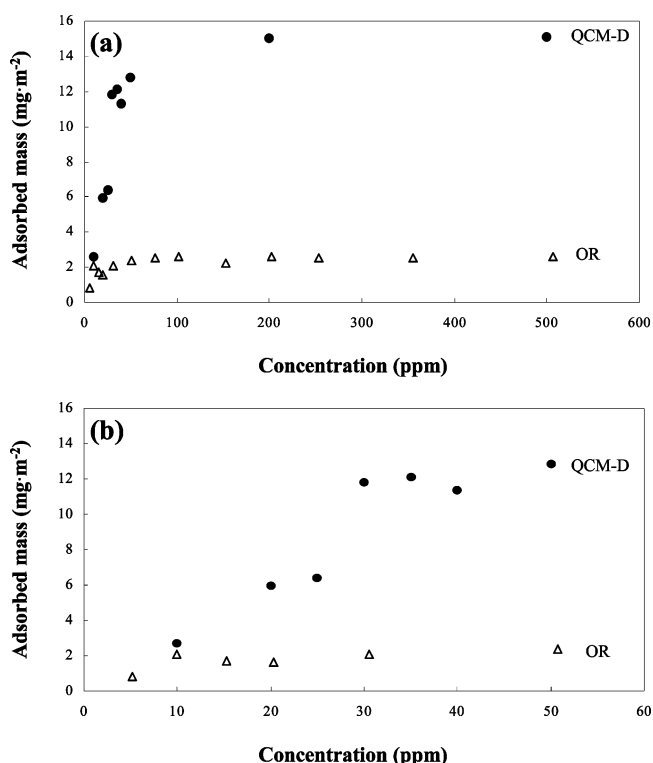


Figure 7. Adsorption isotherms of PDMA_{9X}-PDEA_{2Y} on silica in the presence of 10 mmol·dm⁻³ KNO₃ at pH 9 monitored with either QCM-D (circles) or OR (triangles). (a) Gives the results in the whole range of concentration investigated, while (b) shows the same data in the range of 0–60 ppm.

increasing concentration and reaches a much greater maximum value (15 mg·m⁻²) above 50 ppm copolymer. Furthermore, there is an indication of a “step” at 20–30 ppm in the QCM-D isotherm. Given the cmc value of this particular PDMA-PDEA diblock copolymer, one might predict a conformational change

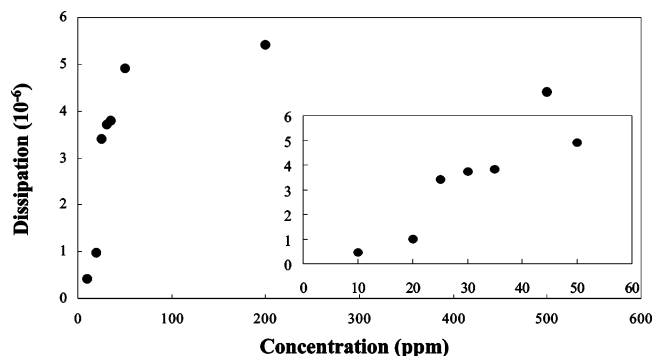


Figure 8. Change in dissipation for adsorption of PDMA_{9X}-PDEA_{2Y} in the presence of 10 mmol·dm⁻³ KNO₃ at pH 9 as a function of the copolymer concentration. The inset shows the same data in the range of 0–60 ppm.

in the adsorbed layer at around this concentration. This likely conformation change is also indicated by the dissipation data, as shown in Figure 8. These data show a well-defined step at 20–30 ppm. On the basis of the adsorption kinetics presented in the preceding section, both the enhanced mass and dissipation values observed above the cmc are thought to be the result of formation of an adsorbed layer with a more extended conformation in the form of surface micelles.⁴⁶

Essentially the same adsorption mechanism, in which diblock copolymers adsorb as unimers below the cmc and as micelles above the cmc, has been proposed on the basis of an ellipsometric study of the adsorption of polystyrene-*block*-PEO (PS-PEO) onto dielectric surfaces in cyclopentane.^{16,17} However, the shape of the adsorption isotherm is quite different to that observed in the present study: the final adsorbed amount of PS-PEO was significantly lower for adsorption from micellar solutions (even at concentrations 10 times higher than the cmc) than for adsorption from unimer solutions. In other words, the maximum amount of adsorption occurred at the cmc. This observation was rationalized as follows. The PS-PEO diblock copolymer must be adsorbed in a configuration that has the hydrophilic PEO blocks bound to the surface while the PS chains extend into the solution phase below the cmc. The driving force for such adsorption is the energetically unfavorable interaction between the PEO blocks and the solvent. On the other hand, above the cmc the adsorbed micelles are required to undergo conformational rearrangement to enable the PEO core micelles to contact the surface sites. Consequently, the adsorbed layer changes to a low-density brush-like conformation, compared with the homogeneous brush-like layer formed at the cmc. In contrast, adsorption of PDMA_{9X}-PDEA_{2Y} is believed to be driven by electrostatic attraction between the cationic copolymer chains and the anionic silica surface. To adopt an extended brush-like conformation, the adsorbed PDMA chains would have to detach from the surface. However, this desorption is most likely not favorable overall, since the formation of a brush layer results in the adsorption of significantly more unimers with a concomitant loss in entropy for the system.¹⁴ Since the PDMA or PDEA blocks both adsorb via an electrostatic charge neutralization with the surface, displacement of one block by another is enthalpically neutral. Hence, the predominant feature of interest is the entropy gained by forming the brush against the entropy lost by attachment to the surface. Clearly, the latter is greater and thus brush formation is not favored for this system.

In our previous investigation using a fluorescent chromophore (pyrene), we found that the PDEA micelle core has hydrophobic character, similar to the hydrophobic micelle cores of conventional surfactants.³² As a result, it is reasonable to suppose that

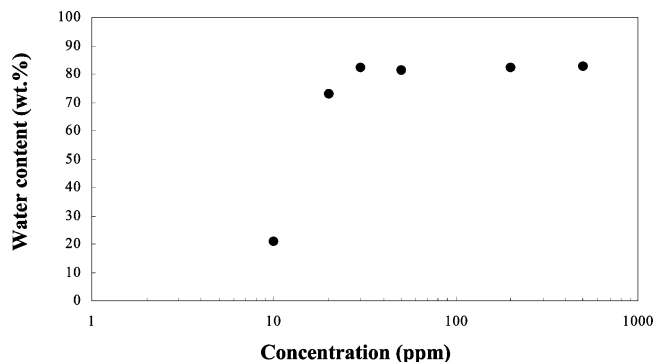


Figure 9. Percentage of water content within PDMA_{9X}-PDEA_{2Y} adsorbed layers on silica as a function of the copolymer concentration.

the entrained water molecules within the diblock copolymer micelles adsorbed onto silica take place principally within the hydrophilic PDMA coronas rather than the hydrophobic PDEA cores. To gain quantitative information on the degree of hydration of this diblock copolymer at the silica/aqueous solution interface, the mass data obtained with QCM-D and OR at given copolymer concentrations are combined. Figure 9 shows the equilibrium percentage of water molecules bound to the copolymers adsorbed on silica, which was calculated using the following relationship

$$\text{Water (wt. \%)} = \frac{(\Gamma_{\text{QCM}} - \Gamma_{\text{OR}})}{\Gamma_{\text{QCM}}} \times 100 \quad (5)$$

where Γ_{QCM} and Γ_{OR} are the adsorbed masses estimated by QCM-D and OR, respectively. The degree of hydration increases sharply in the concentration range of 10–30 ppm and reaches a plateau (82 wt %) at 30 ppm. This concentration is in good agreement with that at which a significant increase in dissipation is observed, suggesting that the degree of hydration is strongly influenced by the conformation of the adsorbed copolymer layers. Previous QCM-D studies have reported that the amount of coupled water within adsorbed layers is 15–40% for a weak polyelectrolyte poly(2-vinylpyridine) (P2VP)³⁷ and 90% for a mussel adhesive protein,³³ respectively. In addition, Plunkett and co-workers³⁵ have shown that the water content ranges from approximately 80% to almost 0% as a function of the charge density on weak polyelectrolytes. This means that the amount of water hydrodynamically coupled within the layers decreases significantly when the adsorbed layer adopts a flat conformation, i.e., when highly charged polyelectrolytes form the adsorbed layer. On the basis of these results, Figure 9 is perfectly reasonable: the high water content above 30 ppm suggests formation of an extended adsorbed layer on silica, while the low percentage observed at 10 ppm indicates a relatively flat conformation. This finding correlates well with the adsorption mechanism derived above.

(IV) Effect of PDMA Chain Length on Adsorption. Figure 10a shows the adsorption isotherms obtained for PDMA₅₄-PDEA₂₄ on silica in the presence of 10 mmol·dm⁻³ KNO₃ at pH 9. The corresponding dissipation values are given in Figure 10b. Comparing these data with the results of PDMA_{9X}-PDEA_{2Y} (Figures 7 and 8), the dissipation of PDMA₅₄-PDEA₂₄ is greater than that of PDMA_{9X}-PDEA_{2Y}, although the difference between the adsorbed masses (in mg·m⁻²) indicated by QCM-D and OR is insignificant for these two diblock copolymers. On the basis of these adsorbed amounts from QCM-D and OR, the degree of hydration of the adsorbed PDMA₅₄-PDEA₂₄ layer is calculated to be 84 wt % ($\Gamma_{\text{QCM}} = 15.8 \text{ mg} \cdot \text{m}^{-2}$ and $\Gamma_{\text{OR}} = 2.5$

TABLE 2: Effect of Copolymer Concentration and Solution pH on the Adsorbed Amount and Dissipation of the Adsorbed PDMA_{9X}-PDEA_{2Y} Layers

| C_p (ppm) | pH 4 | | | | pH 9 | | | |
|-------------|-------------------------------------|--------------------------------------|-------------------------|--------------|-------------------------------------|--------------------------------------|-------------------------|--------------|
| | Γ_{OR} (mg·m ⁻²) | Γ_{QCM} (mg·m ⁻²) | D (10 ⁻⁶) | water (wt %) | Γ_{OR} (mg·m ⁻²) | Γ_{QCM} (mg·m ⁻²) | D (10 ⁻⁶) | water (wt %) |
| 200 | 0.3 | 1.0 | 0.2 | 70 | 2.6 | 15.0 | 5.4 | 83 |
| 500 | 0.3 | 1.5 | 0.9 | 80 | 2.6 | 15.1 | 4.4 | 83 |

mg·m⁻² for a copolymer concentration of 500 ppm), which is comparable to the corresponding degree of hydration of PDMA_{9X}-PDEA_{2Y} adsorbed onto silica (83 wt %) within our experimental resolution. This means that the higher dissipation of the adsorbed PDMA₅₄-PDEA₂₄ layer must be due to other differences, such as the conformation of the adsorbed layer and/or the nature of the surface-adsorbed micelles on silica, rather than due to any difference in the degree of hydration.

As shown in Figure 3, the dissipation of the adsorbed copolymers increases continuously with increasing time, even though the OR data indicate an equilibrium adsorbed amount is attained within a much shorter time frame. This result means that swelling (most likely normal to the interface) of the adsorbed layer may take place during the equilibration period. Since the adsorbed micelles are believed to be principally anchored by the slightly cationic coronal PDMA chains on the anionic silica surface, the degree of flattening upon initial adsorption, and subsequent swelling, is likely to depend on the PDMA chain length. It is reasonable to expect that PDMA_{9X}-PDEA_{2Y} micelles (i.e., longer PDMA chains) will flatten upon initial adsorption to a greater extent than PDMA₅₄-PDEA₂₄ micelles. Consequently, adsorbed micelles comprising PDMA₅₄-PDEA₂₄ chains should swell more readily than those composed of PDMA_{9X}-PDEA_{2Y}. Such a highly expanded conformation for the adsorbed layer will necessarily result in higher dissipation even if both copolymers show the same degree of hydration on silica.

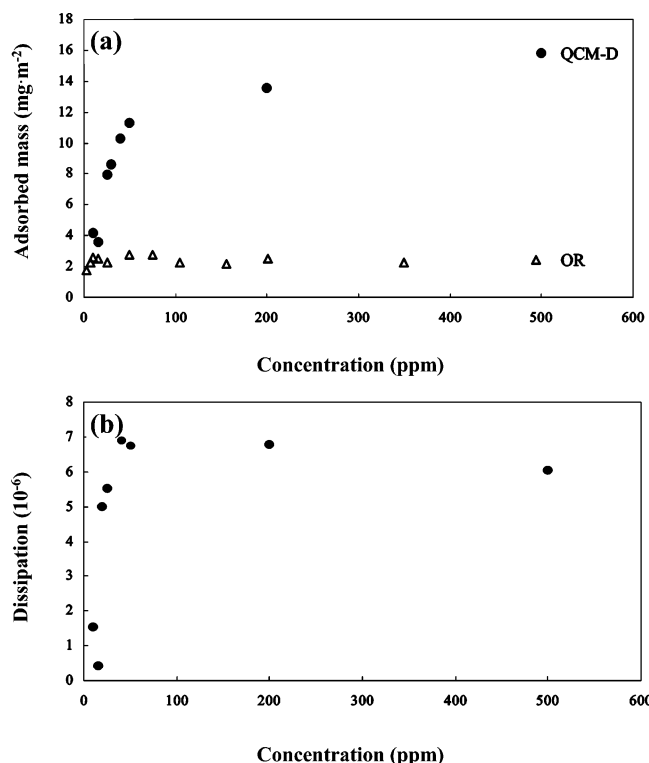


Figure 10. Adsorption isotherms of PDMA₅₄-PDEA₂₄ on silica in the presence of 10 mmol·dm⁻³ KNO₃ at pH 9. (a) Gives the change in the adsorbed mass, while (b) shows the corresponding dissipation change as a function of the copolymer concentration.

Another possible explanation for the higher dissipation of PDMA₅₄-PDEA₂₄ micelles may be their larger micelle size (and higher N_{agg}). By use of the molecular weight of the copolymers (Table 1), the adsorbed OR mass of the PDMA₅₄-PDEA₂₄ copolymer in mol·m⁻² (for example, 0.19 μ mol·m⁻³ at 500 ppm) is calculated to be larger than that of PDMA_{9X}-PDEA_{2Y} (0.14 μ mol·m⁻³ at 500 ppm). This suggests that the adsorbed PDMA₅₄-PDEA₂₄ layers contain many more copolymer chains compared to the adsorbed PDMA_{9X}-PDEA_{2Y} layers. Such a difference is not unexpected, given the greater hydrophobic character of the PDMA₅₄-PDEA₂₄ copolymer. Further investigation is necessary to confirm these hypotheses, for example, by using detailed normal force measurements and/or ellipsometry to measure the adsorbed layer thickness.

(V) Effect of Solution pH. The adsorption behavior of PDMA_{9X}-PDEA_{2Y} onto silica at pH 4 was also investigated. The equilibrium adsorbed amount (monitored with QCM-D and OR) and the corresponding dissipation are given in Table 2. Since protonation of all the tertiary amine groups on both the PDMA and PDEA chains occurs at this pH, this diblock copolymer is molecularly dissolved over the whole range of concentrations studied. Thus interfacial adsorption is restricted to unimers. Adsorption at low pH is therefore limited and corresponds to classical polyelectrolyte adsorption, in which the now highly cationic chains adsorb onto an anionic surface as a relatively flat monolayer. The adsorbed masses of these cationic diblock copolymer chains from 200 and 500 ppm at pH 4 are smaller than that from a unimer solution (10 ppm) at pH 9, although the difference between the corresponding dissipation values is insignificant. In both cases this suggests that the unimers rapidly adopt very flat conformations with large “footprints” (mean area per chain) on the silica surface at pH 4 due to interchain repulsion. In contrast, at pH 9 the electrostatic driving force for adsorption is far weaker, but a higher density is ultimately possible due to the much lower charge density on both blocks. The same finding has been reported for a series of so-called “double hydrophilic” cationic diblock copolymer micelles adsorbed onto silica.¹⁴

Conclusions

The adsorption behavior of a PDMA-PDEA diblock copolymer on silica has been characterized as a function of time, copolymer concentration, and block composition. Individual copolymer chains are adsorbed below the cmc and adopt a flat conformation. The driving force for this adsorption is both electrostatic attraction and the hydrophobic nature of the PDEA blocks. Just above the cmc, adsorption of unimers still dominates the early stages of adsorption due to their faster diffusion toward the silica surface than the much larger micelles. However, once unimer adsorption reaches a pseudoplateau, the present study on silica indicate that rearrangement and/or displacement of the individual adsorbed chains by free micelles occurs. Accordingly, both the equilibrium adsorbed amounts and the corresponding QCM-D dissipation increase steeply just above the cmc. On the other hand, micelles adsorb directly onto silica at copolymer concentrations well above the cmc, even in the early stages of adsorption. The initial adsorbed layer experiences gradual

relaxation during the equilibration period. This rearrangement is believed to be a combination of further copolymer adsorption and subsequent swelling of the adsorbed layer, since the QCM-D dissipation increases continuously during this period.

Acknowledgment. The EPSRC is thanked for the linked research grants GR/S60419 and GR/S60402 awarded to S.P.A. and S.B., respectively. The ARC is thanked for research grant DP0343783. S. Philipon is thanked for assistance with the SLS experiments. V. S. J. Craig and S. M. Notley are thanked for useful discussions. S.P.A. is the recipient of a five-year Royal Society-Wolfson Merit award. S. Y. Liu is thanked for his assistance in preparing one of the three diblock copolymers by ATRP.

References and Notes

- (1) Russell, T. P. *Science* **2002**, 297, 964.
- (2) Yu, K.; Hurd, A. J.; Eisenberg, A.; Brinker, C. J. *Langmuir* **2001**, 17, 7961.
- (3) Chang, J. H.; Wang, L.-Q.; Shin, Y.; Jeong, B.; Birnbaum, J. C.; Exarhos, G. J. *Adv. Mater.* **2002**, 14, 378.
- (4) Smarsly, B.; Xomeritakis, G.; Yu, K.; Liu, N.; Fan, H.; Assink, R. A.; Drewien, C. A.; Ruland, W.; Brinker, C. J. *Langmuir* **2003**, 19, 7295.
- (5) Holmberg, K. J. *Colloid Interface Sci.* **2004**, 274, 355.
- (6) Bronstein, L. M.; Sidorov, S. N.; Valetsky, P. M.; Hartmann, J.; Cölfen, H.; Antonietti, M. *Langmuir* **1999**, 15, 6256.
- (7) Liu, S.; Weaver, J. V. M.; Save, M.; Armes, S. P. *Langmuir* **2002**, 18, 8350.
- (8) Sidorov, S. N.; Bronstein, L. M.; Kabachii, Y. A.; Valetsky, P. M.; Soo, P. L.; Maysinger, D.; Eisenberg, A. *Langmuir* **2004**, 20, 3543.
- (9) Lei, L.; Gohy, J.-F.; Willet, N.; Zhang, J.-X.; Varshney, S.; Jérôme, R. *Macromolecules* **2004**, 37, 1089.
- (10) Zhan, Y.; Mattice, W. L. *Macromolecules* **1994**, 27, 683.
- (11) Walter, H.; Harrats, C.; Müller-Buschbaum, P.; Jérôme, R.; Stamm, M. *Langmuir* **1999**, 15, 1260.
- (12) Mahltig, B.; Walter, H.; Harrats, C.; Müller-Buschbaum, P.; Jérôme, R.; Stamm, M. *Phys. Chem. Chem. Phys.* **1999**, 1, 3853.
- (13) Mahltig, B.; Gohy, J.-F.; Jérôme, R.; Bellmann, C.; Stamm, M. *Colloid Polym. Sci.* **2000**, 278, 502.
- (14) Styrkas, D. A.; Büttin, V.; Lu, J. R.; Keddie, J. L.; Armes, S. P. *Langmuir* **2000**, 16, 5980.
- (15) Mahltig, B.; Gohy, J.-F.; Antoun, S.; Jérôme, R.; Stamm, M. *Colloid Polym. Sci.* **2002**, 280, 495.
- (16) Munch, M. R.; Gast, A. P. *Macromolecules* **1990**, 23, 2313.
- (17) Munch, M. R.; Gast, A. P. *J. Chem. Soc., Faraday Trans.* **1990**, 86, 1341.
- (18) Awan, M. A.; Dimonie, V. L.; Filippov, L. K.; El-Aasser, M. S. *Langmuir* **1997**, 13, 130.
- (19) Abraham, T. *Polymer* **2002**, 43, 849.
- (20) Dijt, J. C.; Cohen-Stuart, M. A.; Hofman, J. E.; Fleer, G. J. *Colloids Surf.* **1990**, 51, 141.
- (21) Hoogeveen, N. G.; Cohen-Stuart, M. A.; Fleer, G. J. *J. Colloid Interface Sci.* **1996**, 182, 133.
- (22) Bijsterbosch, H. D.; Cohen-Stuart, M. A.; Fleer, G. J. *Macromolecules* **1998**, 31, 9281.
- (23) Toomey, R.; Mays, J.; Yang, J.; Tirrell, M. *Macromolecules* **2006**, 39, 2262.
- (24) Liu, S.; Armes, S. P. *Curr. Opin. Colloid Interface Sci.* **2001**, 6, 249.
- (25) Büttin, V.; Billingham, N. C.; Armes, S. P. *Chem. Commun.* **1997**, 671.
- (26) Lee, A. S.; Gast, A. P.; Büttin, V.; Armes, S. P. *Macromolecules* **1999**, 32, 4302.
- (27) Büttin, V.; Armes, S. P.; Billingham, N. C. *Macromolecules* **2001**, 34, 1148.
- (28) Vamvakaki, M.; Unali, G.-F.; Büttin, V.; Boucher, S.; Robinson, K. L.; Billingham, N. C.; Armes, S. P. *Macromolecules* **2001**, 34, 6840.
- (29) Büttin, V.; Armes, S. P.; Billingham, N. C. *Polymer* **2001**, 42, 5993.
- (30) Webber, G. B.; Wanless, E. J.; Büttin, V.; Armes, S. P.; Biggs, S. *Nano Lett.* **2002**, 2, 1307.
- (31) Webber, G. B.; Wanless, E. J.; Armes, S. P.; Tang, Y.; Li, Y.; Biggs, S. *Adv. Mater.* **2004**, 16, 1794.
- (32) Webber, G. B.; Wanless, E. J.; Armes, S. P.; Biggs, S. *Faraday Discuss.* **2005**, 128, 193.
- (33) Höök, F.; Kasemo, B.; Nylander, T.; Fant, C.; Sott, K.; Elwing, H. *Anal. Chem.* **2001**, 73, 5796.
- (34) Stålgren, J. J. R.; Eriksson, J.; Boschkova, K. J. *Colloid Interface Sci.* **2002**, 253, 190.
- (35) Plunkett, M. A.; Claesson, P. M.; Ernstsson, M.; Rutland, M. W. *Langmuir* **2003**, 19, 4673.
- (36) Caruso, F.; Serizawa, T.; Furlong, D. N.; Okahata, Y. *Langmuir* **1995**, 11, 1546.
- (37) Notley, S. M.; Biggs, S.; Craig, V. S. J.; Wågberg, L. *Phys. Chem. Chem. Phys.* **2004**, 6, 2379.
- (38) Liu, S. Y.; Tang, Y. Q.; Weaver, J. V. M.; Billingham, N. C.; Armes, S. P.; Tribe, K. *Macromolecules* **2002**, 35, 6121.
- (39) Rodahl, M.; Höök, F.; Krozer, A.; Brzezinski, P.; Kasemo, B. *Rev. Sci. Instrum.* **1995**, 66, 3924.
- (40) Rodahl, M.; Kasemo, B. *Rev. Sci. Instrum.* **1996**, 67, 3238.
- (41) Sauerbrey, G. Z. *Phys.* **1959**, 155, 206.
- (42) Craig, V. S. J.; Plunkett, M. J. *Colloid Interface Sci.* **2003**, 262, 126.
- (43) Dijt, J. C.; Cohen-Stuart, M. A.; Fleer, G. J. *Adv. Colloid Interface Sci.* **1994**, 50, 79.
- (44) Atkin, R.; Craig, V. S. J.; Biggs, S. *Langmuir* **2000**, 16, 9374.
- (45) Borkovec, M. In *Handbook of Applied Surface and Colloid Chemistry*; Holmberg, K., Eds.; John Wiley & Sons Ltd.: New York, 2001; Chapter 18.
- (46) Sakai, K.; Smith, E. G.; Webber, G. B.; Schatz, C.; Wanless, E. J.; Büttin, V.; Armes, S. P.; Biggs, S. *Langmuir* **2006**, 22, 5328.
- (47) Giacomelli, C.; Men, L. L.; Borsali, R.; Lai-Kee-Him, J.; Brisson, A.; Armes, S. P.; Lewis, A. L. *Biomacromolecules* **2006**, 7, 817.
- (48) Motschmann, H.; Stamm, M.; Toprakcioglu, C. *Macromolecules* **1991**, 24, 3681.
- (49) Amiel, C.; Sikka, M.; Schneider, J. W.; Tsao, Y.-H.; Tirrell, M.; Mays, J. W. *Macromolecules* **1995**, 28, 3125.
- (50) Abraham, T.; Giasson, S.; Gohy, J. F.; Jérôme, R.; Müller, B.; Stamm, M. *Macromolecules* **2000**, 33, 6051.
- (51) Biggs, S.; Proud, A. D. *Langmuir* **1997**, 13, 7202.
- (52) Sakai, K.; Yoshimura, T.; Esumi, K. *Langmuir* **2003**, 19, 1203.
- (53) Dijt, J. C.; Cohen-Stuart, M. A.; Fleer, G. J. *Macromolecules* **1994**, 27, 3219.